

Cell Cycle–Mediated Regulation of Plant Infection by the Rice Blast Fungus ^W

Diane G.O. Saunders, Stephen J. Aves, and Nicholas J. Talbot¹

School of Biosciences, University of Exeter, Exeter EX4 4QD, United Kingdom

To gain entry to plants, many pathogenic fungi develop specialized infection structures called appressoria. Here, we demonstrate that appressorium morphogenesis in the rice blast fungus *Magnaporthe oryzae* is tightly regulated by the cell cycle. Shortly after a fungus spore lands on the rice (*Oryza sativa*) leaf surface, a single round of mitosis always occurs in the germ tube. We found that initiation of infection structure development is regulated by a DNA replication-dependent checkpoint. Genetic intervention in DNA synthesis, by conditional mutation of the Never-in-Mitosis 1 gene, prevented germ tubes from developing nascent infection structures. Cellular differentiation of appressoria, however, required entry into mitosis because *nimA* temperature-sensitive mutants, blocked at mitotic entry, were unable to develop functional appressoria. Arresting the cell cycle after mitotic entry, by conditional inactivation of the Blocked-in-Mitosis 1 gene or expression of stabilized cyclinB-encoding alleles, did not impair appressorium differentiation, but instead prevented these cells from invading plant tissue. When considered together, these data suggest that appressorium-mediated plant infection is coordinated by three distinct cell cycle checkpoints that are necessary for establishment of plant disease.

INTRODUCTION

Many of the most important plant diseases are caused by fungal pathogens that form specialized infection cells to breach the leaf surface. These infection structures are an especially common feature of cereal pathogens, including the causal agents of rust diseases, powdery mildews, and the devastating rice blast disease (Dean, 1997; Tucker and Talbot, 2001). The blast fungus *Magnaporthe oryzae* forms dome-shaped appressoria and uses a turgor-driven process to rupture the cuticle and send a narrow penetration hypha into an underlying plant epidermal cell (for reviews, see Ebbole 2007; Wilson and Talbot, 2009). The appressorium is a differentiated fungal cell with a specialized cell wall rich in chitin and an inner layer lined with melanin (Henson et al., 1999). The melanin layer is essential to *M. oryzae* appressoria because it reduces the porosity of the cell wall, which allows generation of osmotic pressure by accumulation of glycerol and the application of mechanical force at the leaf surface (Howard et al., 1991; De Jong et al., 1997). Interfering with initial plant infection offers one of the best means of controlling the most economically significant plant diseases, and an understanding of fungal infection-related development is therefore essential.

Formation of appressoria involves a switch from polarized hyphal growth to isotropic expansion of the germ tube tip and cellular differentiation of the appressorium. This is followed by turgor generation, reorientation of the axis of polarity, and resumption of polarized fungal growth at the base of the infection

cell, rupturing the host cuticle. Following entry into the leaf, *M. oryzae* undergoes a further developmental switch to form specialized invasive hyphae, which secrete effector proteins and sequester nutrients from living host cells (Kankanala et al., 2007).

To initiate appressorium development, the fungus responds to a set of inductive cues, including surface hardness, hydrophobicity, cuticular wax, and the absence of exogenous nutrients (Ebbole, 2007). How each of these signals is perceived is not clear, but the process involves at least one G-protein-coupled receptor, Pth11, and cognate G- α and G- $\beta\gamma$ -subunit proteins (reviewed in Wilson and Talbot, 2009). Adenylate cyclase-mediated generation of cAMP and protein kinase A are necessary for efficient appressorium morphogenesis (Choi and Dean, 1997; Xu et al., 1997; Adachi and Hamer, 1998; Thines et al., 2000), and a mitogen-activated protein kinase pathway composed of the Mst11, Mst7, and Pmk1 protein kinases is essential for appressorium formation and subsequent invasive growth (Zhao et al., 2005). However, how these signaling pathways are connected to the developmental biology of the fungus as it undergoes the morphogenetic transitions to form differentiated infection structures is unclear.

In this study, we set out to explore the relationship between cell cycle regulation and infection structure development in the rice blast fungus. The cell cycle is pivotal to cellular differentiation in multicellular eukaryotes, which must synchronize cell division to form specific tissues and organs effectively (Kipreos, 2005; Théry and Bornens, 2006; Cools and De Veylder, 2009). The switch between isotropic and polarized growth in fungi is also intimately linked to cell cycle regulation in yeasts and filamentous and dimorphic fungal species (Momany, 2002; Whiteway and Bachewich, 2007; Steinberg and Perez-Martin, 2008). We therefore hypothesized that cell cycle regulation would be likely to provide control points for infection structure development by *M. oryzae*. Previously, we showed that mitosis is necessary for appressorium formation and infection-associated autophagy

¹ Address correspondence to n.j.talbot@exeter.ac.uk.

The author responsible for distribution of materials integral to the findings presented in this article in accordance with the policy described in the Instructions for Authors (www.plantcell.org) is: Nicholas J. Talbot (n.j.talbot@exeter.ac.uk).

^WOnline version contains Web-only data.

www.plantcell.org/cgi/doi/10.1105/tpc.109.072447

during plant infection (Veneault-Fourrey et al., 2006), providing the first indication of cell cycle regulation of this process. In this study, we set out to use a combination of live-cell imaging and gene functional analysis to determine how such cell cycle regulation of infection-related development might operate and, in particular, to define the individual cell cycle checkpoints necessary for appressorium morphogenesis and subsequent plant infection. We report here that the key step in initiating infection structure development in *M. oryzae* is entry into S-phase, which causes formation of an incipient infection cell at the germ tube tip. Cellular differentiation of this terminal swelling requires mitosis to have occurred, with mitotic entry marking the regulatory commitment point for appressorium maturation. We further present evidence that subsequent progression through mitosis is dispensable for appressorium maturation but is essential for plant infection. When considered together, this suggests that there are three pivotal cell cycle checkpoints that operate in the rice blast fungus to allow it to gain entry to its host plant.

RESULTS

Mitosis Always Precedes Appressorium Development in *M. oryzae*

To investigate nuclear division and migration during appressorium formation, we performed live-cell imaging of *M. oryzae* expressing a histone H1-enhanced red fluorescent protein (RFP; tdTomato) fusion (Shaner et al., 2004) and β -tubulin-synthetic green fluorescent protein (sGFP) fusion, as shown in Figure 1 and Supplemental Movie 1 online. Following spore germination, a polarized germ tube was formed and microtubules aligned parallel to its longitudinal axis (Figure 1A). Mitosis occurred 4 to 6 h later with an influx of β -tubulin:sGFP into the nucleus as the spindle formed (see Supplemental Movie 1 online; Figure 1B). Astral microtubules were evident during spindle elongation and rapid separation of chromosomes (Figure 1B). Following mitosis, one daughter nucleus migrated to the swollen germ tube tip, while the other returned to the original conidial cell. The germ tube tip swelled prior to mitosis and continued to develop, increasing in diameter upon receipt of the daughter nucleus (Figure 1C). The three nuclei that remained in the spore were then broken down by autophagic cell death (Veneault-Fourrey et al., 2006) with a single nucleus remaining in the appressorium as shown in Figure 1A.

Initiation of Appressorium Morphogenesis Is Regulated at S-Phase

To investigate the importance of cell cycle progression to appressorium development, we applied the DNA synthesis inhibitor hydroxyurea (HU) to conidia of *M. oryzae*. Following addition of HU, germinating conidia arrested predominantly with undifferentiated germ tubes, rather than incipient appressoria, as shown in Figures 2A and 2C. This is in contrast with perturbation of the cell cycle in *M. oryzae* with either benomyl or a *nimA*^{E37G} mutation, both of which cause a late G2 arrest but allow the formation of swollen germ tube tips (Veneault-Fourrey et al., 2006). We reasoned that DNA replication (S-phase) might be

necessary for formation of the terminal swelling that later develops into an appressorium. To test this idea, we generated a mutant that was affected in DNA replication but that would still allow mitotic entry. In the filamentous fungus *Aspergillus nidulans*, the temperature-sensitive *nimO18* mutant (for never in mitosis) is unable to replicate DNA, although aberrant segregation of chromatin can occur, leading to cells advancing into mitosis with unreplicated DNA at the restrictive temperature (James et al., 1999). NimO is functionally related to *Saccharomyces cerevisiae* Dbf4p, the regulatory subunit of the Cdc7p-Dbf4p kinase complex, which is required for Cdc7p kinase activity and initiation of DNA replication (Jackson et al., 1993). We identified an *M. oryzae* gene, *NIM1*, which putatively encodes a protein of 651 amino acids with 31% sequence identity to *A. nidulans* NimO (see Supplemental Figure 1 online). Analysis of the Nim1 sequence revealed a BRCT domain (residues 116 to 166 [e-value 0.32]) that is characteristic of cell cycle regulators involved in the DNA damage checkpoint (Bork et al., 1997), the Dbf4 M motif (residues 241 to 369 [e-value 9.1e-45]), and a zinc finger (residues 582 to 630 [e-value 2e-26]), all of which are conserved in Dbf4-related proteins (Ogino et al., 2001).

We generated a temperature-sensitive mutant of *NIM1* by making a *nim1*^{I327E} allele, identical to the mutation found in the thermo-labile *nimO18* mutant of *A. nidulans* (James et al., 1999), and introduced this into the *M. oryzae* *H1:RFP*-expressing strain of Guy11 by targeted allelic replacement. Transformants were selected that showed a severe hyphal growth defect at the restrictive temperature of 32°C, and growth was only partially restored by subsequent incubation at 24°C (Figure 2B). Following DNA gel blot analysis, transformants with a single targeted replacement of the *nim1*^{I327E} allele were identified, and two transformants (2 and 41) were selected each containing the I327E substitution.

We determined the frequency of nuclear division and appressorium development in the *nim1*^{I327E} mutants and the isogenic *H1:RFP* strain. Appressorium development was significantly reduced in *nim1*^{I327E} mutants (*t* test; *P* < 0.001) compared with the wild type, and conidia instead formed undifferentiated germlings when incubated at the semirestrictive temperature (Figures 2C and 2D). However, we still observed nuclear division in *nim1*^{I327E} strains (Figure 2C), consistent with the reported phenotype of *A. nidulans nimO18* mutants (James et al., 1999). The *M. oryzae nim1*^{I327E} mutant was able to initiate numerous rounds of aberrant nuclear division, and we reasoned that this was likely to be due to the partial inactivation of the Nim1 protein at 29°C (higher temperatures affected appressorium morphogenesis, as reported previously [Veneault-Fourrey et al., 2006]). We interpreted the *nim1*^{I327E} phenotype as being consistent with segregation of unreplicated, or partially replicated, chromatin. To test this idea, we added the DNA synthesis inhibitor HU to germinating *nim1*^{I327E} conidia. We consistently observed a postmitotic growth arrest phenotype in which nuclei still divided in *nim1*^{I327E} mutants exposed to HU. By contrast, the wild-type *H1:RFP* strain always arrested growth prior to mitosis (Figure 2E). This strongly indicates that *nim1*^{I327E} mutants are capable of circumventing the DNA replication checkpoint, thereby enabling nuclear division to take place in the absence of DNA replication (James et al., 1999). High-resolution imaging of the chromatin status of *nim1*^{I327E} cells in the presence of HU was consistent

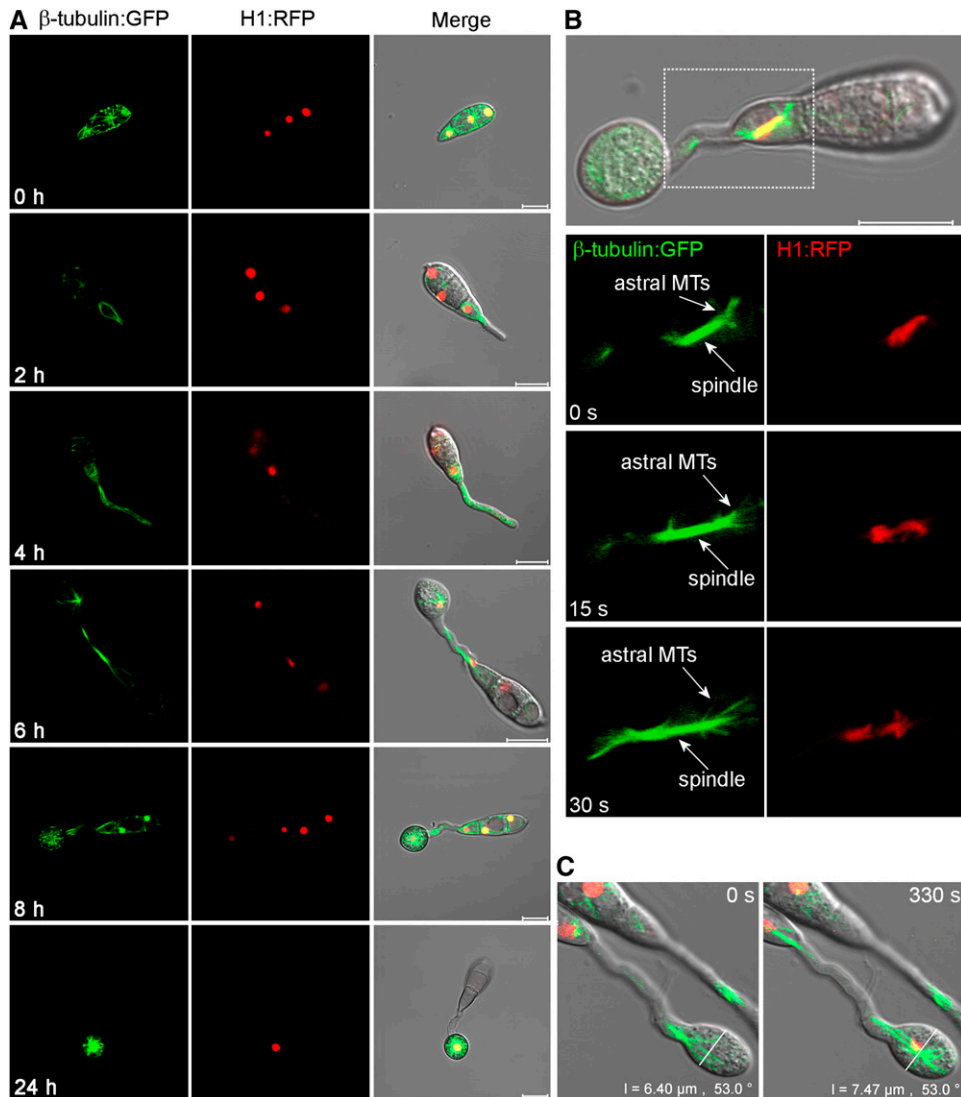


Figure 1. Live-Cell Imaging of Microtubule Dynamics and Nuclear Division in *M. oryzae* during Germination and Appressorium Development.

(A) Time series of micrographs showing nuclear division during appressorium development in *M. oryzae*. The *grg(p):H1:RFP* and *ccg1(p):bm1:sGFP* gene fusion vectors were introduced into the *M. oryzae* wild-type strain Guy-11. Nuclei (red) and microtubules (green) were observed during conidial germination and appressorium development in *M. oryzae*.

(B) Astral microtubules were observed during mitotic spindle elongation and the concurrent rapid separation of chromosomes. MTs, microtubules.

(C) Continued expansion in diameter of the incipient appressorium during mitotic division. Bars = 10 μm .

with this conclusion (see Supplemental Figure 2 online). Importantly, *nim1^{I327E}* mutants were unable to initiate appressorium development or conidial autophagic cell death in the presence of HU (Figure 2F), demonstrating that successful execution of DNA replication is necessary for initiation of appressorium morphogenesis by the rice blast fungus.

Mitotic Entry Is Both Necessary and Sufficient for Appressorium Development

Previously, we showed that blocking the cell cycle at mitotic entry (G2-M) was sufficient to prevent appressorium development by *M.*

oryzae (Veneault-Fourrey et al., 2006). This conclusion was based on the fact that temperature-sensitive *nimA^{E37G}* mutants were unable to make mature appressoria at the restrictive temperature (Veneault-Fourrey et al., 2006). *M. oryzae* NimA encodes a functional homolog of the *A. nidulans* NimA protein kinase, which is essential for mitosis (Osmani et al., 1991). We noted that *nimA^{E37G}* mutants were able to form swollen germ tube tips but could not develop mature, melanized infection cells, preventing *nimA^{E37G}* mutants from causing plant disease (see Supplemental Figure 3A online). We therefore set out to determine at which stage *M. oryzae* germlings became committed to appressorium differentiation by attempting to block mitosis at a point subsequent to mitotic entry.

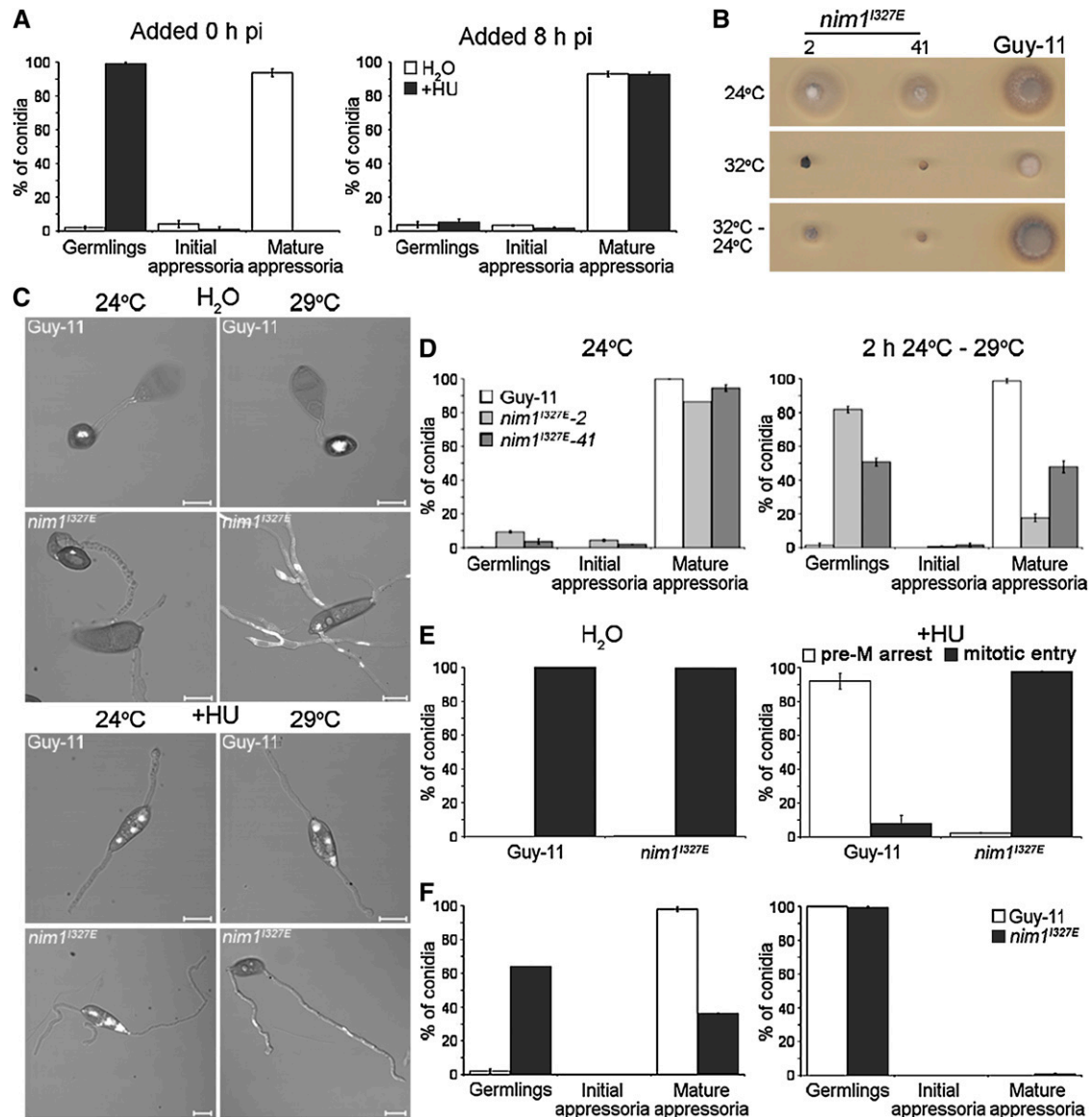


Figure 2. DNA Replication in *M. oryzae* Is Necessary for Initiation of Appressorium Development.

(A) The effect of chemical inhibition of DNA replication on appressorium development in *M. oryzae*. Water (white bars) or the DNA synthesis inhibitor HU (+HU, black bars) was added (200 mM) to conidial suspensions of the *H1::RFP* strain, 0 or 8 h postinoculation (hpi). The percentage of conidia developing undifferentiated germ tubes (germlings), swollen germ tube tips (initial appressoria), and differentiated infection cells (mature appressoria) was recorded after 8 h.

(B) Temperature sensitivity of the *nim1*^{1327E} mutant of *M. oryzae*; two putative *nim1*^{1327E} transformants (2 and 41) and Guy-11 were incubated at a permissive temperature of 24°C or a restrictive temperature of 32°C for 4 d. Restoration of hyphal growth was assessed by incubation for a further 3 d at 24°C.

(C) Representative images of the *nim1*^{1327E} mutant during appressorium development, in the presence (bottom panels) or absence (top panels) of HU; *nim1*^{1327E} and Guy-11 germinating conidia were fixed and stained with the DNA-specific stain 4',6-diamidino-2-phenylindole 24 h postinoculation, following incubation at 24 or 29°C. Bars = 10 μm.

(D) Bar charts to show frequency of appressorium development in *M. oryzae nim1*^{1327E}. Conidial suspensions of *nim1*^{1327E} transformants 2 and 41 were incubated on hydrophobic surfaces at 24 or 29°C. The percentage of conidia developing undifferentiated germ tubes (germlings), swollen germ tube tips (initial appressoria), or differentiated infection cells (mature appressoria) was recorded after 24 h.

(E) Bar charts to show the frequency of germinating conidia displaying a premitotic arrest (pre-M arrest; white bars) or the ability to progress into mitosis uninhibited (mitotic entry; black bars).

(F) HU was added to *nim1*^{1327E} and Guy-11 conidia at 0 h and nuclear division and appressorium development assessed 24 h later following incubation at 24°C (left bar chart) or 29°C (right bar chart). All graphs represent two biological and three technical replicate observations of 100 germinating conidia. Error bars are 1 SE.

In *A. nidulans*, the blocked in mitosis *bimE7* mutant has been described, which arrests cells in mitosis in a pre-anaphase state (Osmani et al., 1988). The *A. nidulans* BimE protein is homologous to the large subunit of the *S. cerevisiae* anaphase-promoting complex (APC; Peters et al., 1996). We identified an *M. oryzae* gene, *BIM1*, from the *M. oryzae* genome database (Dean et al., 2005), which showed 35% sequence identity with *A. nidulans* BimE. Sequence analysis of Bim1 revealed three proteasome/cyclosome repeat regions (residues 1140 to 1174 [e-value 0.78], residues 1185 to 1223 [e-value 0.37], and residues 1328 to 1362 [e-value 0.3]), consistent with the protein acting as a component of the multisubunit APC in *M. oryzae* (see Supplemental Figure 4 online). To test this relationship, we introduced *BIM1* into the *S. cerevisiae* thermosensitive mutant, *apc1-ΔC* (Winzeler et al., 1999). Expression of *M. oryzae BIM1* allowed the mutant to grow at the restrictive temperature, consistent with *M. oryzae* Bim1 protein acting as a component of the APC (Figure 3A). We then sequenced the previously uncharacterized *A. nidulans bimE7* allele, which revealed a point mutation altering a Gln residue to a premature stop codon at position 1966. A corresponding *bim1^{F1763*}* allele was constructed, introduced into *M. oryzae* by homologous recombination, and transformants selected that were unable to grow at 32°C (Figure 3B). Following DNA gel blot analysis, the allelic replacement of *BIM1* was confirmed by amplification of the locus and DNA sequencing (data not shown).

To test the effect of the *bim1^{F1763*}* mutation on appressorium development, we selected two independent transformants and first quantified their abilities to complete mitosis, as shown in Figure 3C. The wild-type *H1:RFP* strain progressed through mitosis normally at both temperatures, resulting in degradation of the three conidial nuclei and retention of a single nucleus in the appressorium (Figures 3C and 3D). By contrast, *bim1^{F1763*}* mutants arrested in mitosis, or displayed a range of nuclear migration defects, consistent with impairment of mitosis (Figures 3C and 3D; Osmani et al., 1988). The phenotypes observed suggest that Bim1 acts as a regulator of mitotic progression, consistent with its role as a component of the APC, which catalyzes ubiquitination of anaphase-specific inhibitors (Cohen-Fix et al., 1996), targeting them for proteasome degradation and thereby facilitating mitotic progression. Transferring germinating conidia to 29°C at later times had a less dramatic effect on nuclear division and migration because the nonsynchronously germinating conidia had increasingly passed through mitosis before transfer to the semirestrictive temperature (for a full quantitative analysis, see Supplemental Figure 3B online).

Importantly, *bim1^{F1763*}* mutants were consistently able to develop mature, melanized appressoria even at the restrictive temperature (Figure 3E), indicating that arrest of the cell cycle after mitotic entry has no effect on appressorium morphogenesis. We conclude that mitotic entry is therefore both necessary and sufficient for the induction of appressorium differentiation in *M. oryzae*.

To analyze further this phenotype, we decided to carry out epistasis analysis of the *bim1^{F1763*}* and *nimA^{E37G}* mutations by constructing a double mutant. In *A. nidulans* when the G2-specific *nimA5* and *bimE7* mutations are combined, *nimA5 bimE7* double mutant cells enter mitosis and arrest in a pre-anaphase state, a phenotype indistinguishable from that of the

bimE7 single mutant (Osmani et al., 1991). We quantified nuclear division in a *M. oryzae nimA^{E37G} bim1^{F1763*}* double mutant and observed that nuclear division always arrested at mitotic entry, as observed in *nimA^{E37G}* single mutants (see Supplemental Figure 5 online). These results demonstrate that although the *A. nidulans* NimA and BimE proteins appear functionally conserved in *M. oryzae*, the epistatic relationship between them is clearly distinct.

Appressoria formed normally in *bim1^{F1763*}* mutants, and we were therefore interested to find out whether these were functional infection cells capable of initiating rice blast disease. We therefore infected the rice (*Oryza sativa*) seedlings of cultivar CO-39 at permissive and semipermissive temperatures. We found that disease symptoms caused by *bim1^{F1763*}* mutants were significantly reduced at the semirestrictive temperature of 29°C (Figure 3F; two-sample *t* test assuming equal variances, $t = 9.27$, $df = 10$, $P < 0.05$), although no effect was observed at the permissive temperature of 24°C when compared with the wild-type strain, Guy 11 (Figure 3F; two-sample *t* test assuming equal variances, $t = 0.94$, $df = 16$, $P > 0.05$). Cytological analysis on rice or sterile onion epidermal layers indicated that appressoria of *bim1^{F1763*}* mutants were unable to elaborate penetration hyphae at the semipermissive temperature of 29°C. When considered together, our results suggest that mitotic entry is sufficient for appressorium morphogenesis but that plant infection depends on completion of mitosis during appressorium morphogenesis by the rice blast fungus.

Expression of Stabilized Forms of the *M. oryzae* B-Type Cyclin Genes Prevents Mitotic Exit

To test our hypothesis that mitotic entry was sufficient to enable appressorium development by *M. oryzae*, we decided to carry out an alternative strategy to block the cell cycle prior to mitotic exit. To do this, we identified two putative *M. oryzae* cyclin B-encoding genes, *CYC1* and *CYC2*, which showed similarity to cyclin B homologs from other fungi (see Supplemental Figure 6 online). We analyzed the predicted amino acid sequences of *CYC1* and *CYC2* to identify destruction box consensus sequences (RXLLXXXXN) essential for targeting cyclin B for ubiquitin-mediated degradation during mitotic exit (reviewed in Hochstrasser, 1996). We reasoned that by removing these sequences and expressing the resulting alleles in *M. oryzae*, we would be able to prevent mitotic exit, thus providing an alternative means of establishing the cell cycle commitment point for appressorium development.

We identified and removed the destruction box consensus sequences from *CYC1* and *CYC2*, to create the *CYC1^{-D1D2}* and *CYC2^{-D2}* alleles, respectively (see Supplemental Figure 6 online). The modified dominant alleles were then placed under the *ICL1* promoter from the isocitrate lyase-encoding gene of *M. oryzae* (Wang et al., 2003), to enable induction of gene expression by acetate, and introduced into the fungus. We identified transformants carrying single copies of the *CYC1^{-D1D2}* and *CYC2^{-D2}* alleles, respectively, by DNA gel blot analysis and DNA sequencing. We then quantified the ability of these strains to undergo nuclear division in the presence or absence of acetate, as shown in Figure 4. The wild-type *H1:RFP* strain progressed through mitosis normally and, following autophagy of the spore,

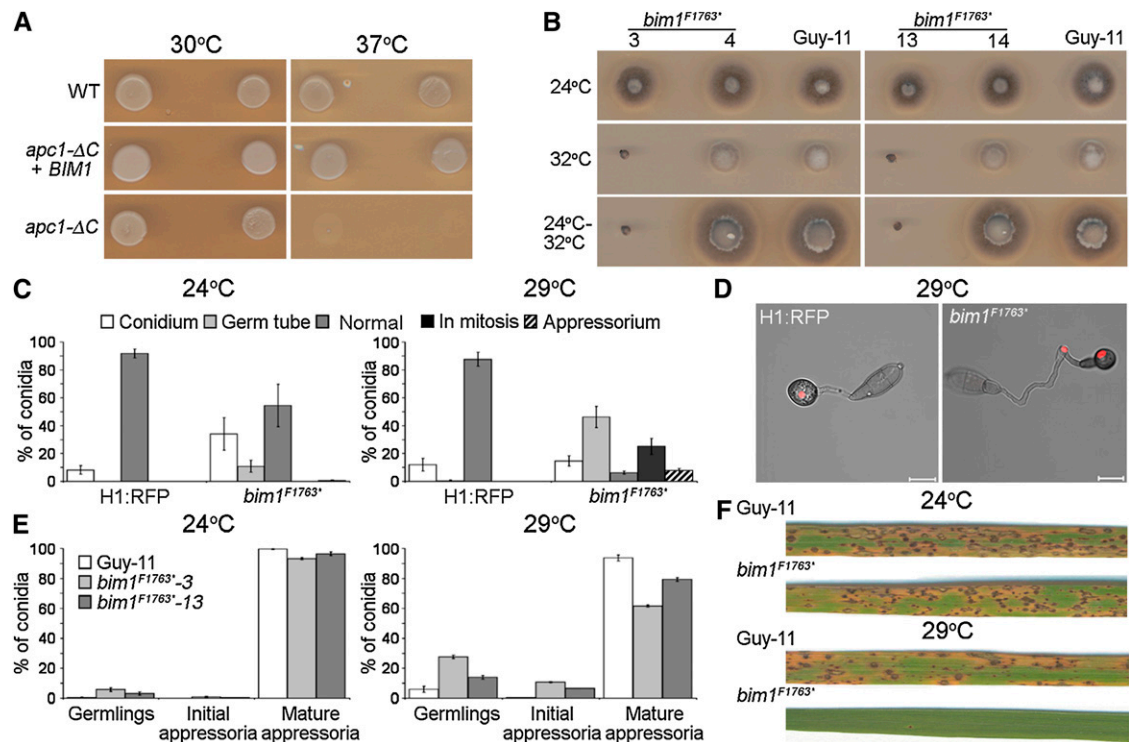


Figure 3. The *M. oryzae* *bim1^{F1763*}* Mutant Forms Appressoria but Is Unable to Cause Plant Disease.

(A) *M. oryzae* *BIM1* is a functional homolog of *S. cerevisiae* *APC1*. The *M. oryzae* *BIM1* gene coding sequence under the control of the *GAL1* promoter was introduced into the *S. cerevisiae* *apc1-ΔC* mutant. Induced expression of *BIM1* restored growth of *apc1-ΔC* at 37°C.

(B) Temperature sensitivity of the *bim1^{F1763*}* mutant of *M. oryzae*. Hyphal growth analysis of *bim1^{F1763*}* mutant transformants (3 and 13), ectopic transformants (4 and 14), and Guy-11 after incubation at 24 or 32°C for 4 d. Restoration of hyphal growth was assessed by incubation for a further 3 d at 24°C.

(C) Bar charts to illustrate nuclear distribution during appressorium development in *bim1^{F1763*}*. Nuclear position was recorded following appressorium development of the *bim1^{F1763*}* mutant and the *H1:RFP* wild-type strain after 24 h at 29°C. Nuclei were scored as being both retained in the spore (Conidium), arrested in the germ tube (Germ tube), blocked in mitosis (Mitosis), both migrating to the developing infection cell (Appressorium), or progressing normally through mitosis, resulting in a single nucleus in the appressorium and degradation of the remaining three nuclei (Normal).

(D) Representative images to show nuclear distribution during appressorium formation of the *bim1^{F1763*}* mutant and *H1:RFP* strain, after 24 h at 29°C.

(E) Quantitative analysis of appressorium development of the *bim1^{F1763*}* mutant after incubation of germinating conidia at 24 or 29°C for 24 h. All graphs represent two biological and three technical replicate observations of 100 germinating conidia. Error bars are 1 SE.

(F) *M. oryzae* *bim1^{F1763*}* mutants are unable to cause rice blast disease. Leaves from rice cultivar CO-39 inoculated with 5×10^4 spores mL⁻¹ of *bim1^{F1763*}* and Guy 11. Rice plants were incubated initially for 24 h at either 24 or 29°C. All plants were then transferred to 24°C and leaves were harvested 5 d later.

contained a single nucleus in each appressorium (Figures 4B and 4C). By contrast, in the presence of acetate, we found that nuclear division was disrupted during appressorium development in both the *CYC1^{-D1D2}* and *CYC2^{-D1}* strains, which also expressed *H1:RFP*, and they displayed either a complete block in mitosis or a range of nuclear distribution phenotypes in which nuclei failed to migrate to the appressorium or conidium or migrated together. The impairment of mitotic exit was most pronounced in the *CYC1^{-D1D2-5}* mutant, in which 41% of germinated conidia arrested nuclear migration with two daughter nuclei remaining very close together in the germ tube (Figure 4B). By contrast, we observed hyphal growth defects of *CYC2^{-D1}* strains when incubated in the presence of acetate (Figure 4D) compared with the wild type or *CYC1^{-D1D2}* strains. This indicates that *CYC2* may be more important during vegetative hyphal

growth, suggesting stage-specific functions for the two cyclins in *M. oryzae*.

The ability of *CYC1^{-D1D2}* and *CYC2^{-D1}* strains to develop appressoria was analyzed in the presence and absence of acetate. Appressoria developed normally in both *CYC1^{-D1D2}* and *CYC2^{-D1}* strains in the presence of acetate (Figure 4A), suggesting that mitotic exit is not necessary for appressorium differentiation and providing further evidence that mitotic entry is the commitment point for appressorium maturation by the rice blast fungus.

DISCUSSION

In this study, we set out to explore the relationship between cell cycle progression and infection structure formation by a plant

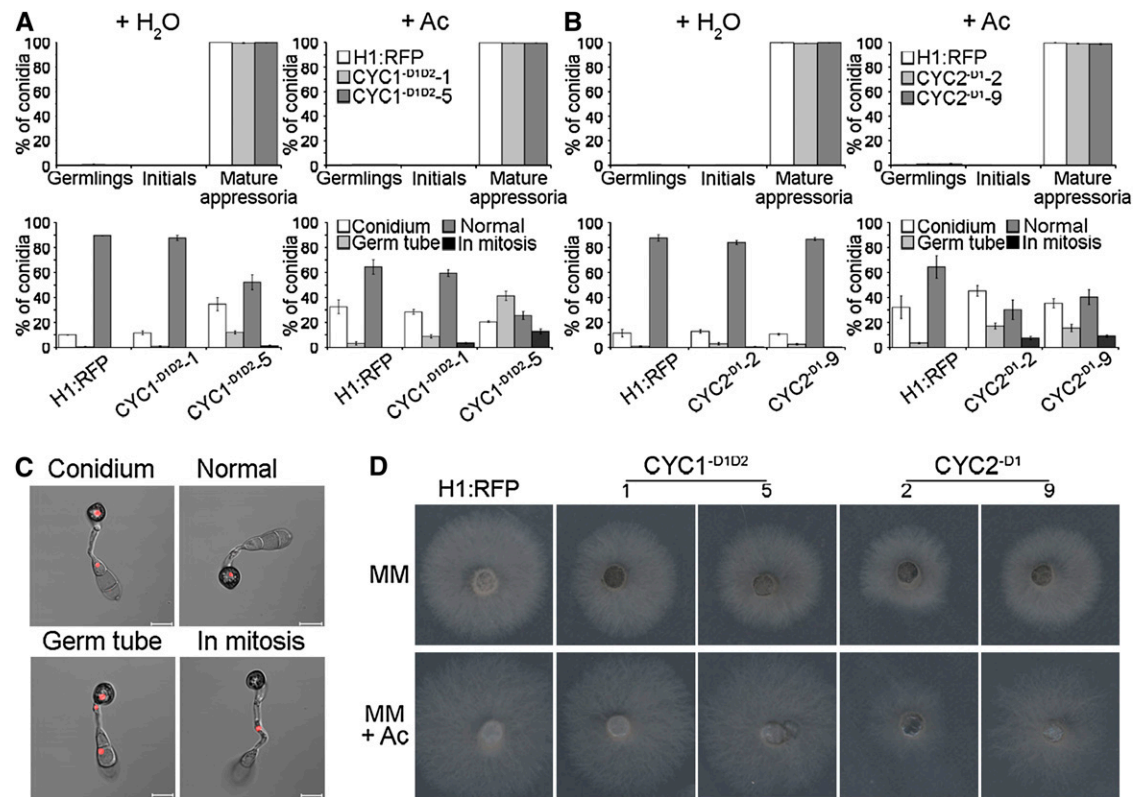


Figure 4. Expression of Stabilized Cyclin B Proteins in *M. oryzae* Inhibits Mitotic Exit but Does Not Prevent Appressorium Morphogenesis.

(A) Bar charts to show frequency of appressorium development (top panel) and nuclear distribution patterns (bottom panel) in two independent *CYC1-D1D2* transformants (1 and 5). Appressorium development and nuclear distribution during appressorium morphogenesis were assessed in the presence or absence of 50 mM sodium acetate (Ac) 24 h postinoculation to induce expression of stabilized cyclins. For key, see legend to Figure 3. **(B)** Bar charts to show frequency of appressorium development and nuclear distribution patterns in two *CYC2-D1* transformants (2 and 9). Germinating conidia were incubated to allow appressorium development in the presence or absence of 50 mM Ac and observed 24 h later. All graphs represent two biological and three technical replicate observations of 100 germinating conidia. Error bars are 1 SE.

(C) Representative images of *CYC1-D1D2*, *CYC2-D1*, and *H1:RFP* strains in the presence or absence of Ac during appressorium morphogenesis. Nuclei were scored as being both retained in the spore (Conidium), arrested in the germ tube (Germ tube), blocked in mitosis (in mitosis), or progressing normally through mitosis, resulting in a single nucleus in the appressorium and degradation of the remaining three nuclei (Normal).

(D) Phenotypic analysis of *CYC1-D1D2* and *CYC2-D1* expression on hyphal growth in *M. oryzae*. Plugs of mycelium (5 mm diameter) from *ICL1(p):CYC1-D1D2*, *ICL1(p):CYC2-D1*, and *H1:RFP* were incubated in the presence (MM + Ac) or absence (MM) of 50 mM Ac. Hyphal growth was assessed 4 d later. Bars = 10 μ m.

pathogenic fungus. Previous evidence had suggested that mitosis was needed for appressorium formation by *M. oryzae* (Veneault-Fourrey et al., 2006) but did not reveal which stage of the cell cycle governed initiation and differentiation of infection structure formation. We reasoned that by constructing conditional mutants, impaired at each stage of the cell cycle, and combining these with quantitative cytological analysis of fluorescently tagged strains of *M. oryzae*, we would be able to determine the most likely regulation points for infection-related development.

S-Phase Regulation of Infection Structure

Our first conclusion is that entry into S-phase is critical for regulating initiation of appressorium development. The evidence to support this idea is based on analysis of the *nim1^{327E}* mutant, which is impaired in DNA replication but still undergoes nuclear

division. Even when exposed to HU, which completely blocked DNA replication, *nim1^{327E}* mutants showed a postmitotic arrest phenotype, indicating that the mutation circumvents the DNA replication checkpoint, enabling nuclear division to take place in the absence of DNA replication. Because these mutants were unable to initiate appressorium development, the regulation point for initiating appressorium development must occur prior to mitosis and depend on a checkpoint operating at S-phase (Figure 5). Consistent with this, time-lapse microscopy of mitosis showed that the swollen germ tube tip always developed prior to mitosis, providing the destination for one of the daughter nuclei, which rapidly migrates into the germ tube apex (see Supplemental Movie 1 online).

The inductive cues for appressorium development, such as surface hydrophobicity, cuticular wax, and the absence of nutrients, must therefore be perceived at a very early stage following

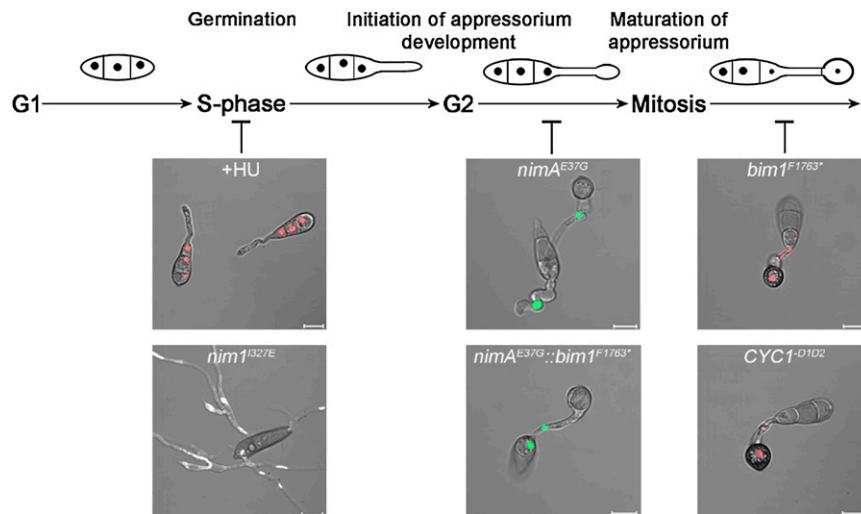


Figure 5. Model for the Regulation of Infection Structure Development by Cell Cycle Progression in *M. oryzae*.

Entry into S-phase leads to initiation of appressorium development in the rice blast fungus. Arresting S-phase with HU or *nim1*^{I327E} mutation prevents germ tubes from swelling and initiating appressorium formation. Entry into mitosis is both necessary and sufficient for appressoria to fully differentiate, as demonstrated by the phenotypes of the *nimA*^{E37G} and *nimA*^{E37G}*bim1*^{F1763*} mutants. Mitotic progression and exit are not necessary for appressoria to mature but may regulate repolarization and subsequent disease development. Bars = 10 μ m.

spore germination on the rice leaf and stimulate the nucleus to pass rapidly from G1-S, as a necessary prerequisite for appressorium formation. By contrast, previous work has shown that when *M. oryzae* spores are incubated under noninductive conditions, they undergo mitosis much later (after 6 to 8 h), and this does not lead to terminal swelling of the germ tube or to degeneration of the nuclei within the spore (Veneault-Fourrey et al., 2006). Therefore, the inductive properties of the rice leaf cause a fundamental change in cell cycle regulation that is necessary for appressorium formation. How such an S-phase checkpoint operates is not clear, but one possibility is through the action of the Pmk1 mitogen-activated protein kinase (MAPK) cascade, which is essential for appressorium development (Zhao et al., 2005). Δ *pmk1* mutants do not form appressoria and instead develop undifferentiated germ tubes on rice leaves. Interestingly, successive rounds of mitosis occur in germ tubes of Δ *pmk1* mutants, suggesting that the MAPK may be involved in regulating S-phase and initiation of appressorium formation. Pmk1 is functionally related to the Fus3/Kss1 MAPKs in yeast, which are involved in the pheromone signaling pathway and also modulate the cell cycle through the action of Far1, which induces a cell cycle arrest that is required for yeast mating to occur (McKinney and Cross, 1995). The Pmk1 MAPK module consists of three protein kinases, Mst11, Mst7, and Pmk1, held together by a scaffold protein Mst50, which interacts with Mst11 and Mst7 (Park et al., 2006). Mst50 also interacts with the Rho GTPase, Cdc42, an essential polarity marker, providing evidence that the pathway regulates the switch between polarized and isotropic growth that is necessary for appressorium formation. Our results suggest that this process is likely to be integrated with cell cycle regulation. Cyclic AMP signaling has also been shown to be essential for the initiation of appressorium development in *M. oryzae* (Choi and Dean, 1997; Adachi and Hamer, 1998) and may

also operate upstream of the cell cycle regulation points identified in this study. Consistent with this idea, we found that addition of cAMP (up to 10 mM) to germinating conidia on hydrophobic plastic surfaces did not rescue the phenotype of *nim1*^{I327E} mutants or the ability of HU to suppress appressorium formation (data not shown).

Mitosis Is Necessary and Sufficient for Appressorium Maturation in *M. oryzae*

The second major finding from this study is that entry into mitosis represents a commitment point for appressorium morphogenesis by *M. oryzae*. Previous analysis of the *nimA*^{E37G} mutant showed that blocking the cell cycle prior to mitosis prevented appressoria from developing properly and becoming fully differentiated, melanized infection structures (Veneault-Fourrey et al., 2006). This study shows that blocking the cell cycle at later stages, such as anaphase or mitotic exit, has no effect on appressorium formation; infection structures form normally and become melanized. This strongly suggests that the checkpoint regulating cellular differentiation operates at the G2-M boundary, marking the point at which *M. oryzae* becomes committed to making an appressorium.

Two lines of evidence support this conclusion. First, the *bim1*^{F1763*} mutation caused a severe impairment in mitosis at a semipermissive temperature, which was evident by our observation of failure of nuclei to separate correctly or undergo nuclear migration. Strikingly, we observed that in spite of a clear mitotic block in *bim1*^{F1763*} mutants, appressoria formed normally, consistent with mitotic entry being sufficient for their development.

Our second test of this idea was to block mitotic exit, which we performed by regulated expression of stabilized forms of the two *M. oryzae* cyclin B genes, *CYC1* and *CYC2*, lacking their

inherent destruction box consensus sequences. We found that *CYC1-D1D2* and *CYC2-D1* strains both displayed mitotic exit phenotypes, which is consistent with stabilized expression of truncated cyclin B genes in *U. maydis* (Garcia-Muse et al., 2003). There were, however, stage-specific differences in the phenotypes of the mutants, with *CYC1-D1D2* strains showing more severe impairment in mitotic exit during infection-related development and *CYC2-D1* strains severely affecting vegetative growth. In the human pathogenic fungus *Candida albicans*, the Clb2 cyclin has been shown to be essential for vegetative growth, while Clb4 negatively regulates pseudohyphal growth, consistent with differential expression of B-type cyclins being important in the regulation of polarized hyphal growth (Bensen et al., 2005). Similarly the *U. maydis* B-type cyclins fulfill distinct developmental roles, with Clb2 acting as a negative regulator of budding, independent of Clb1 (Garcia-Muse et al., 2003). Impairment of mitotic exit in *CYC1-D1D2* and *CYC2-D1* strains did not, however, affect appressorium formation in *M. oryzae*, providing independent support for the hypothesis that entry into mitosis is sufficient for appressorium formation.

Our final, and more tentative, conclusion is that completion of mitosis during appressorium morphogenesis is an essential prerequisite to plant infection. This is based on the fact that although *bim1^{F1763*}* mutants form appressoria normally, they are unable to cause rice blast disease. This suggests that completion of mitosis is necessary for repolarization of the penetration hypha at the base of the appressorium to bring about cuticle rupture. We propose that the nucleus within the appressorium has to progress to G1 phase to allow the infection structure to be functionally competent. What we cannot tell at this time is whether a further round of DNA replication is also necessary to allow repolarization of the appressorium, with the nucleus passing into G2, prior to penetration peg development. Analysis of conidial germination, however, suggests that germ tube emergence occurs while the nucleus is still in G1 and progression through to G2 only occurs after polar growth has been established (Veneault-Fourrey et al., 2006). If the same holds true for emergence of the penetration peg at the base of the appressorium, then this would suggest that repolarization of the appressorium is also a G1-regulated event and, therefore, logically requires the previous mitosis to have been completed, although this will require further investigation.

In summary, this study has identified an interdependent relationship between the morphological transitions associated with plant infection and cell cycle progression exhibited by *M. oryzae* (presented in Figure 5). Initiation of appressorium morphogenesis is dependent on execution of DNA replication. Mitotic entry is both necessary and sufficient to initiate appressorium maturation in *M. oryzae*, and exit from mitosis appears to be required for plant infection.

METHODS

Fungal Strains, Growth Conditions, and Infection Structure Development Assays

All isolates of *Magnaporthe oryzae* (Couch and Kohn, 2002; formerly *M. grisea*) used in this study were stored in the laboratory of N.J.T. See

Supplemental Table 1 online for strains generated in this work. Growth and maintenance of *M. oryzae*, media composition, nucleic acid extraction, transformation, and plant infection assays were all as described previously (Talbot et al., 1993). Conidial germination and development of appressoria were monitored over time on hydrophobic borosilicate glass cover slips (Fisher Scientific) using a method adapted from Hamer et al. (1988). Conidial suspensions at 5×10^4 conidia mL⁻¹ were inoculated onto cover slips, incubated at 24°C, and the frequency of conidial germination and appressorium development recorded 24 h later, unless otherwise stated.

Live-Cell Imaging of Nuclei and Cytoskeletal Components of *M. oryzae*

Details of the construction of the *H1:RFP* (tdTomato) and *β-tubulin:sGFP* gene fusion vectors are given in Supplemental Methods online. Constructs were introduced into the *M. oryzae* wild-type strain Guy-11 (Leung et al., 1988) and transformants selected by DNA gel blots. At least two independent transformants were investigated for all experiments and were demonstrated to be fully pathogenic and grow normally (see Supplemental Figure 7 online). All images of conidial germination and appressorium development were recorded using a Zeiss LSM510 Meta confocal laser scanning microscope system. Slides were prepared for processing by sealing cover slip appressorium preparations to a slide with petroleum jelly (Vaseline; Unilever). Blue diode (405 nm), argon (458, 477, 488, and 504 nm), and helium-neon (543 and 633 nm) lasers were used to excite fluorochromes and all images recorded following examination under the ×63 oil objective. Offline image analysis was performed using the LSM image browser (Zeiss) or MetaMorph 7.5 (Molecular Devices). The confocal laser scanning microscope multitrack setting was used to enable synchronized image acquisition.

For nuclear staining, conidial suspensions of *M. oryzae* were prepared on cover slips and inverted onto 100-μL aliquots of fixative solution (3.7% formaldehyde, 50 mM phosphate buffer, pH 7, and 0.2% Triton X-100) and incubated at room temperature for 5 min. Cover slips were then submerged in 20 mL water for 5 min and stained by submersion in 1 μg mL⁻¹ 4',6-diamidino-2-phenylindole (Sigma-Aldrich) for 5 min. Cover slips were washed a second time in 20 mL water for 5 min and allowed to air dry. Germinating conidia were then mounted in 10 μL Na-PO₄, pH 8, 50% glycerol (v/v), and 0.1% propyl-gallate (Fluka).

Identification of Putative Cell Cycle Regulator Genes in *M. oryzae*

Putative *M. oryzae* cell cycle regulators were identified by interrogation of the sixth release of the annotated genome sequence of *M. oryzae* from the Broad Institute (<http://www.broad.mit.edu/annotation/fungi/magnaporthe>) using the BLASTP algorithm (Altschul et al., 1990). Protein sequences were aligned using ClustalW (<http://www.ebi.ac.uk/clustalw/>) and shaded using Boxshade v 2.01 (http://www.ch.embnet.org/software/BOX_form.html). For detailed protein sequence analysis, we used the Pfam database (<http://www.sanger.ac.uk/Software/Pfam/>). Details of construction for the allelic replacement vectors for *nim1^{Δ327E}*, *bim1^{F1763*}*, and *nimA^{E37G}bim1^{F1763*}* mutant generation are given in Supplemental Methods online.

M. oryzae BIM1 Complementation of the *Saccharomyces cerevisiae* *apc1-ΔC* Mutant

Complementation of the *S. cerevisiae* *apc1* temperature-sensitive (ts) mutant, *apc1-ΔC* (Winzeler et al., 1999), was performed by amplifying the *BIM1* coding sequence from *M. oryzae* RNA using the Titanium One-Step RT-PCR kit (BD Biosciences) and cloning into pYES2 (Invitrogen) using primers 5BimE-EcoRI and 3BimE-HindII, as shown in Supplemental Table 2 online. The *S. cerevisiae* strain *MATa apc1-ΔC::KanMX4*

(YNL171c::KanMX4) was provided by Claus Zachariae (University of Copenhagen, Denmark) and used for yeast transformation using the Yeastmarker system (Clontech). Six putative transformants were selected and grown in 50 mL YPD with 2% glucose for 16 h in a shaking incubator at 30°C and 230 rpm with the *apc1-ΔC* mutant and an isogenic wild-type strain. The cultures were then used to inoculate two sets of YPD plates supplemented with 2% glucose and 2% galactose, respectively. Successful complementation of *BIM1* in *S. cerevisiae* strain *apc1-ΔC* was assessed by observing the ability of putative transformants to restore growth of the *apc1-ΔC* strain at 37°C.

Identification of the *Aspergillus nidulans* *bimE7* Mutation

The full-length 6.2-kb *A. nidulans* *bimE* gene was amplified from both the *A. nidulans* *bimE7* strain (kindly provided by Steve Osmani, Ohio State University, Columbus, OH) and a wild-type strain A89 (Fungal Genetics Stock Center). Both *bimE* alleles were sequenced (Eurofins MWG Operon) and a single mutation identified in *bimE7*, which altered a Gln residue in the amino acid sequence to introduce a premature stop codon at position 1966. This was verified by separate amplification of the two alleles and further DNA sequence analysis.

Identification of Putative *M. oryzae* B-Type Cyclins

Two *M. oryzae* putative cyclin B-encoding genes, *CYC1* and *CYC2*, were identified from the *M. oryzae* genome database, with the *Ustilago maydis* B-type cyclins, Clb1 and Clb2. The 1.5-kb *M. oryzae* cyclin B gene *CYC1* and 1.9-kb cyclin B homolog *CYC2* were amplified from RNA using the Titanium One-Step RT-PCR kit (BD Biosciences) and introduced into pCR 2.1-TOPO (primers 5CyclinB1, 3CyclinB1, 5CyclinB2, and 3CyclinB2). Modified *CYC1* and *CYC2* alleles in which the destruction box consensus sequences were removed, as described in the Supplemental Methods online, were introduced into the *M. oryzae* *H1:RFP* strain. Regulated expression was performed in the presence of acetate; for details, see Supplemental Methods online.

Accession Numbers

Sequence data from this article can be found in the GenBank/EMBL databases under the following accession numbers: *M. oryzae* *NIM1* (MG00597), *M. oryzae* *BIM1* (MG03314), *M. oryzae* *CYC1* (MG05646), *M. oryzae* *CYC2* (MG07065), *M. oryzae* *NIMA* (MG03026), *A. nidulans* Histone H1 vector pMF280 (AY598429), *A. nidulans* *BimE* (AN2772), *U. maydis* *Clb1* (AY260969), *U. maydis* *Clb1* (AY260970), *S. cerevisiae* *APC1* (CAA96060), *C. albicans* *CLB2* (U40430), *C. albicans* *CLB4* (AF094507), *A. nidulans* *NimE* (X64602), *S. pombe* *Cig2* (S67490), *S. pombe* *Cdc13* (X12557), *S. cerevisiae* *CLB2* (X62319), *S. cerevisiae* *CLB3* (X69425), *S. cerevisiae* *CLB4* (X69426), *S. cerevisiae* *CLB5* (X70435), and *S. cerevisiae* *CLB6* (X70436).

Supplemental Data

The following materials are available in the online version of this article.

Supplemental Figure 1. Alignment of the Predicted *M. oryzae* Nim1 Amino Acid Sequence with *A. nidulans* NimO and *S. cerevisiae* Dbf4.

Supplemental Figure 2. High-Resolution Micrographs of Chromatin Status of *M. oryzae* Arrested at Different Stages of the Cell Cycle.

Supplemental Figure 3. Mitotic Entry Is Sufficient for *M. oryzae* Appressorium Maturation, and *bim1^{F1763}* Inhibits Nuclear Division during Appressorium Morphogenesis.

Supplemental Figure 4. Alignment of the Predicted *M. oryzae* Bim1 Amino Acid Sequence with *A. nidulans* BimE and *S. cerevisiae* Apc1.

Supplemental Figure 5. *M. oryzae* *nim^{AE37G}:bim1^{F1763}* Displays a Typical *nim^{AE37G}* Phenotype during Appressorium Development.

Supplemental Figure 6. Alignment of the Predicted *M. oryzae* B-Type Cyclins with Characterized B-Type Cyclins from *A. nidulans*, *U. maydis*, *C. albicans*, *S. cerevisiae*, and *S. pombe*, Which Act Specifically at the G2-Mitotic Transition.

Supplemental Figure 7. Construction of the *grg(p):H1:RFP* and *ccg1(p):bm1:sGFP* Gene Fusion Vectors and Expression in *M. oryzae*.

Supplemental Table 1. *M. oryzae* Strains Generated in This Study.

Supplemental Table 2. Detailed Information of the Primers Used in This Study.

Supplemental Methods.

Supplemental Movie 1. Live-Cell Imaging of Mitotic Division during Appressorium Development in *M. oryzae*.

ACKNOWLEDGMENTS

This work was supported by a grant to N.J.T. from the Biotechnology and Biological Sciences Research Council and a graduate fellowship for D.G.O.S from the University of Exeter. We thank Steve James (Gettysburg College, Gettysburg, PA) and Steve Osmani (Ohio State University, Columbus, OH) for kindly providing *Aspergillus* mutants and for valuable discussions, Gero Steinberg and M.J. Kershaw (University of Exeter) for help with figure and movie preparation, and Richard Wilson (University of Nebraska, Lincoln, NE) for helpful discussions.

Received October 26, 2009; revised January 4, 2010; accepted February 8, 2010; published February 26, 2010.

REFERENCES

- Adachi, K., and Hamer, J.E. (1998). Divergent cAMP signaling pathways regulate growth and pathogenesis in the rice blast fungus *Magnaporthe grisea*. *Plant Cell* **10**: 1361–1373.
- Altschul, S.F., Gish, W., Miller, W., Myers, E.W., and Lipman, D.J. (1990). Basic local alignment search tool. *J. Mol. Biol.* **215**: 403–410.
- Bensen, E.S., Clemente-Blanco, A., Finley, K.R., Correa-Borders, J., and Berman, J. (2005). The mitotic cyclins Clb2p and Clb4p affect morphogenesis in *Candida albicans*. *Mol. Biol. Cell* **16**: 3387–3400.
- Bork, P., Hofmann, K., Bucher, P., Neuwald, A.F., Altschul, S.F., and Koonin, E.V. (1997). A superfamily of conserved domains in DNA damage-responsive cell cycle checkpoint proteins. *FASEB J.* **11**: 68–76.
- Choi, W., and Dean, R.A. (1997). The adenylate cyclase gene *MAC1* of *Magnaporthe grisea* controls appressorium formation and other aspects of growth and development. *Plant Cell* **9**: 1973–1983.
- Cohen-Fix, O., Peters, J.M., Kirschner, M.W., and Koshland, D. (1996). Anaphase inhibition in *Saccharomyces cerevisiae* is controlled by the APC-dependent degradation of the anaphase inhibitor Pds1p. *Genes Dev.* **10**: 3081–3093.
- Cools, T., and De Veylder, L. (2009). DNA stress checkpoint control and plant development. *Curr. Opin. Plant Biol.* **12**: 23–28.
- Couch, B.C., and Kohn, L.M. (2002). A multilocus gene genealogy concordant with host preference indicates segregation of a new species, *Magnaporthe oryzae*, from *M. grisea*. *Mycologia* **94**: 683–693.
- Dean, R.A. (1997). Signal pathways and appressorium morphogenesis. *Annu. Rev. Phytopathol.* **35**: 211–234.
- Dean, R.A., et al. (2005). The genome sequence of the rice blast fungus *Magnaporthe grisea*. *Nature* **434**: 980–986.

- De Jong, J.C., McCormack, B.J., Smirnov, N., and Talbot, N.J.** (1997). Glycerol generates turgor in rice blast. *Nature* **389**: 244–245.
- Ebbole, D.J.** (2007). *Magnaporthe* as a model for understanding host-pathogen interactions. *Annu. Rev. Phytopathol.* **45**: 437–456.
- Garcia-Muse, T., Steinberg, G., and Perez-Martin, J.** (2003). Pheromone-induced G₂ arrest in the phytopathogenic fungus *Ustilago maydis*. *Eukaryot. Cell* **2**: 494–500.
- Hamer, J.E., Howard, R.J., Chumley, F.G., and Valent, B.** (1988). A mechanism for surface attachment in spores of a plant pathogenic fungus. *Science* **239**: 288–290.
- Henson, J.M., Butler, M.J., and Day, A.W.** (1999). The dark side of the mycelium: Melanin of phytopathogenic fungi. *Annu. Rev. Phytopathol.* **37**: 447–471.
- Hochstrasser, M.** (1996). Ubiquitin-dependent protein degradation. *Annu. Rev. Genet.* **30**: 405–439.
- Howard, R.J., Ferrari, M.A., Roach, D.H., and Money, N.P.** (1991). Penetration of hard substrates by a fungus employing enormous turgor pressures. *Proc. Natl. Acad. Sci. USA* **88**: 11281–11284.
- Jackson, A.L., Pahl, P.M., Harrison, K., Rosamond, J., and Sclafani, R.A.** (1993). Cell cycle regulation of the yeast Cdc7 protein kinase by association with the Dbf4 protein. *Mol. Cell. Biol.* **13**: 2899–2908.
- James, S.W., Bullock, K.A., Gygas, S.E., Kraynack, B.A., Matura, R.A., MacLeod, J.A., McNeal, K.K., Prasauckas, K.A., Scacheri, P.C., Shenefiel, H.L., Tobin, H.M., and Wade, S.D.** (1999). *nimO*, an *Aspergillus* gene related to budding yeast *Dbf4*, is required for DNA synthesis and mitotic checkpoint control. *J. Cell Sci.* **112**: 1313–1324.
- Kankanala, P., Czymmek, K., and Valent, B.** (2007). Roles for rice membrane dynamics and plasmodesmata during biotrophic invasion by the blast fungus. *Plant Cell* **19**: 706–724.
- Kipreos, E.T.** (2005). *C. elegans* cell cycles: Invariance and stem cell divisions. *Nat. Rev. Mol. Cell Biol.* **6**: 766–776.
- Leung, H., Borromeo, E.S., Bernardo, M.A., and Notteghem, J.L.** (1988). Genetic analysis of virulence in the rice blast fungus *Magnaporthe grisea*. *Genetics* **78**: 1227–1233.
- McKinney, J.D., and Cross, F.R.** (1995). FAR1 and the G1 specific specificity of cell cycle arrest by mating factor in *Saccharomyces cerevisiae*. *Mol. Cell. Biol.* **15**: 2509–2516.
- Momany, M.** (2002). Polarity in filamentous fungi: Establishment, maintenance and new axes. *Curr. Opin. Microbiol.* **5**: 580–585.
- Ogino, K., Takeda, T., Matsui, E., Iiyama, H., Taniyama, C., Arai, K., and Masai, H.** (2001). Bipartite binding of a kinase activator activates Cdc7-related kinase essential for S phase. *J. Biol. Chem.* **276**: 31376–31387.
- Osmani, A.H., McGuire, S.L., and Osmani, S.A.** (1991). Parallel activation of the *nimA* and *p34^{cdc2}* cell cycle-regulated protein-kinases is required to initiate mitosis in *Aspergillus nidulans*. *Cell* **67**: 283–291.
- Osmani, S.A., Engle, D.B., Doonan, J.H., and Morris, N.R.** (1988). Spindle formation and chromatin condensation in cells blocked at interphase by mutation of a negative cell cycle control gene. *Cell* **52**: 241–251.
- Park, G., Xue, C., Zhao, X., Kim, Y., Orbach, M., and Xu, J.-R.** (2006). Multiple upstream signals converge on the adaptor protein Mst50 in *Magnaporthe grisea*. *Plant Cell* **18**: 2822–2835.
- Peters, J.M., King, R.W., Hoog, C., and Kirschner, M.W.** (1996). Identification of BIME as a subunit of the anaphase-promoting-complex. *Science* **274**: 1199–1201.
- Shaner, N.C., Campbell, R.E., Steinbach, P.A., Giepmans, B.N.G., Palmer, A.E., and Tsien, R.Y.** (2004). Improved monomeric red, orange and yellow fluorescent proteins derived from *Discosoma* sp. red fluorescent protein. *Nat. Biotechnol.* **22**: 1567–1572.
- Steinberg, G., and Perez-Martin, J.** (2008). *Ustilago maydis*, a new fungal model system for cell biology. *Trends Cell Biol.* **18**: 61–67.
- Talbot, N.J., Ebbole, D.J., and Hamer, J.E.** (1993). Identification and characterization of *MPG1*, a gene involved in pathogenicity from the rice blast fungus *Magnaporthe grisea*. *Plant Cell* **5**: 1575–1590.
- Théry, M., and Bornens, M.** (2006). Cell shape and cell division. *Curr. Opin. Cell Biol.* **18**: 648–657.
- Thines, E., Weber, R.W.S., and Talbot, N.J.** (2000). MAP kinase and protein kinase A-dependent mobilization of triacylglycerol and glycogen during appressorium turgor generation by *Magnaporthe grisea*. *Plant Cell* **12**: 1703–1718.
- Tucker, S.L., and Talbot, N.J.** (2001). Surface attachment and pre-penetration stage development by plant pathogenic fungi. *Annu. Rev. Phytopathol.* **39**: 385–417.
- Veneault-Fourrey, C., Barooah, M., Egan, M., Wakely, G., and Talbot, N.J.** (2006). Cell cycle-regulated autophagic cell death is necessary for plant infection by the rice blast fungus. *Science* **312**: 580–583.
- Wang, Z., Thornton, C.R., Kershaw, M.J., Debaio, L., and Talbot, N.J.** (2003). The glyoxylate cycle is required for temporal regulation of virulence by the plant pathogenic fungus *Magnaporthe grisea*. *Mol. Microbiol.* **47**: 1601–1612.
- Whiteway, M., and Bachewich, C.** (2007). Morphogenesis in *Candida albicans*. *Annu. Rev. Microbiol.* **61**: 529–553.
- Wilson, R.A., and Talbot, N.J.** (2009). Under pressure: investigating the biology of plant infection by *Magnaporthe oryzae*. *Nat. Rev. Microbiol.* **7**: 185–195.
- Winzeler, E.A., et al.** (1999). Functional characterization of the *S. cerevisiae* genome by gene deletion and parallel analysis. *Science* **285**: 901–906.
- Xu, J.R., Urban, M., Sweigard, J.A., and Hamer, J.E.** (1997). The *CPKA* gene of *Magnaporthe grisea* is essential for appressorial penetration. *Mol. Plant Microbe Interact.* **10**: 187–194.
- Zhao, X., Kim, Y., Park, G., and Xu, J.R.** (2005). A mitogen-activated protein kinase cascade regulating infection-related morphogenesis in *Magnaporthe grisea*. *Plant Cell* **17**: 1317–1329.

Cell Cycle Mediated Regulation of Plant Infection by the Rice Blast Fungus

Diane G.O. Saunders, Stephen J. Aves and Nicholas J. Talbot

PLANT CELL 2010;22;497-507; originally published online Feb 26, 2010;

DOI: 10.1105/tpc.109.072447

This information is current as of April 23, 2010

Supplemental Data	http://www.plantcell.org/cgi/content/full/tpc.109.072447/DC1
References	This article cites 42 articles, 21 of which you can access for free at: http://www.plantcell.org/cgi/content/full/22/2/497#BIBL
Permissions	https://www.copyright.com/ccc/openurl.do?sid=pd_hw1532298X&issn=1532298X&WT.mc_id=pd_hw1532298X
eTOCs	Sign up for eTOCs for <i>THE PLANT CELL</i> at: http://www.plantcell.org/subscriptions/etoc.shtml
CiteTrack Alerts	Sign up for CiteTrack Alerts for <i>Plant Cell</i> at: http://www.plantcell.org/cgi/alerts/ctmain
Subscription Information	Subscription information for <i>The Plant Cell</i> and <i>Plant Physiology</i> is available at: http://www.aspb.org/publications/subscriptions.cfm